

Nanostructured polymers for photonics

We review recent progress in the development of polymer nanostructured materials with periodic structures and compositions having applications in photonics and optical data storage. This review provides a brief description of the microfabrication and self-assembly methods used for the production of polymer materials with periodic structures, and highlights the properties and applications of photonic materials derived from block copolymers, colloid crystals, and microfabricated polymers. We conclude with a summary of current and future research efforts and opportunities in the development of polymer materials for photonic applications.

Chantal Paquet¹ and Eugenia Kumacheva^{2-4,*}

¹Steele Institute for Molecular Sciences, National Research Council, 100 Sussex Drive, Ottawa, Ontario, K1A 0R6, Canada

²Department of Chemistry, University of Toronto, 80 Saint George Street, Toronto, Ontario M5S 3H6, Canada

³Department of Chemical Engineering and Applied Chemistry, University of Toronto, 200 College Street, Toronto, Ontario M5S 3E5, Canada

⁴Institute of Biomaterials and Biomedical Engineering, University of Toronto, 4 Taddle Creek Road, Toronto, Ontario M5S 3G9, Canada

E-mail: ekumache@chem.utoronto.ca

In the last decade, photonics has emerged as a major interdisciplinary field of science and technology with a focus on the transport and manipulation of light. Rapid progress in photonics has been achieved because of continuous advances in nanotechnologies, materials science, optics, physics, and the rapid development of microfabrication techniques. In particular, interaction of light with materials possessing a periodic modulation in their structure has led to a range of interesting and sometimes unique effects, which have shown promising applications in the production of Bragg mirrors, switches, filters, superprisms, waveguides, and optical resonators.

Polymers play an important role in the development of materials for photonics. Polymers are relatively inexpensive, can be functionalized to

achieve required optical, electronic, or mechanical properties, and have demonstrated compatibility with various patterning methods. Polymers can be used as materials for photonic applications in several ways. First, polymers in themselves can possess useful optical properties such as electroluminescence, photoluminescence, or nonlinear optical properties¹. Second, polymers can act as matrices for optically active species, e.g. for dyes, liquid crystals (LCs), quantum dots, or metal nanoparticles². Third, polymers possessing topographic and/or compositional patterns can coherently scatter light³. Finally, polymer templates are routinely used for producing photonic materials⁴.

We highlight recent research efforts, challenges, and opportunities in the development of polymer nanostructured materials for applications in photonics and optical data storage. The review is limited

to materials whose photonic properties originate from a periodic modulation in structure and/or composition. Discussion of polymers for fiber-optics, optically active polymers with a homogeneous structure, and polymer-based templates for the production of photonic materials is omitted for lack of space.

The review begins with an outline of the general application-related properties of polymer photonic crystals, followed by a concise description of the strategies used for fabricating polymer materials with periodic structures. Polymer photonic materials derived from colloid crystals are described before progress in developing block copolymer materials with photonic properties is summarized. Polymer photonic materials produced by microfabrication techniques are described, and a summary and outlook are given at the end.

Polymer photonic crystals

Photonic crystals are materials in which a periodic spatial modulation in the refractive index leads to coherent scattering of light and alters the modes of propagation of light of wavelengths commensurate with the length scale of the periodicity^{5,6}. Figs. 1a–1c illustrate the structures of one-, two-, and three-dimensional photonic crystals. In particular, three-dimensional photonic crystals with a sufficiently high value of refractive index mismatch, Δn , between the constituent phases possess a full photonic bandgap, where light of a specific wavelength range is inhibited from propagating in all directions. Photonic crystals obtained from polymers possess an intrinsically low value of Δn originating from the relatively low refractive index of polymers, and as a result these materials do not possess a full bandgap. Nevertheless, polymer photonic crystals (PPCs) reveal some of the unique optical

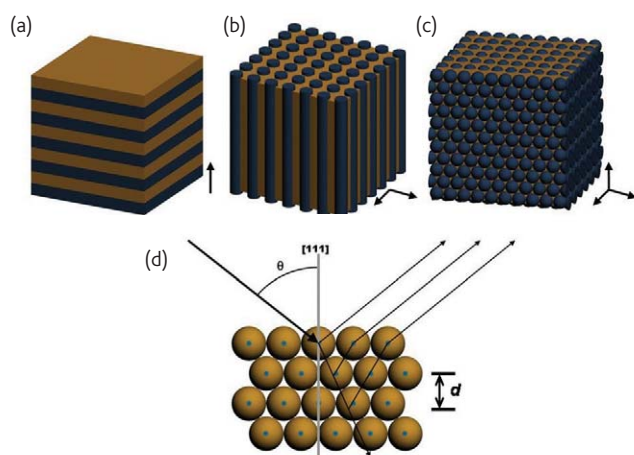


Fig. 1 Schematics of (a) one-, (b) two-, and (c) three-dimensional photonic crystals. The arrows to the right of the crystals show the direction in which a periodic modulation in the refractive index exists. (d) Incident light with a wavelength predicted by a modified Bragg equation (eq 1) undergoes diffraction when propagating through a photonic crystal. The wavelength of light that is coherently scattered is centered on λ_{sb} , and can be estimated from the angle of incidence, θ , the effective refractive index of the PPC, n_{eff} , and the periodicity of the structure, d .

properties that are characteristic of full photonic bandgap materials. For example, PPCs suppress propagation of light in specific directions and wavelength ranges (referred to later in the text as 'stopbands'), which forms the basis of new polymeric optical devices as described below⁷.

Coherent scattering of light

The wavelength of light, λ_{sb} , that is coherently scattered by a three-dimensional PPC (Fig. 1d) can be related to the material periodicity, d , via an approximation of Bragg's and Snell's laws as:

$$k\lambda_{sb} \approx 2d(n_{eff}^2 - \sin^2 \theta)^{1/2} \quad (1)$$

where k is the order of diffraction, n_{eff} is the effective refractive index of the PPC, and θ is the angle of incidence of light with respect to the normal of the PPC. The dependence of λ_{sb} on material characteristics (i.e. d and n_{eff}) allows PPCs to function as sensors. For example, the introduction of analytes or solvents^{8–12}, the action of electric fields^{13–15}, or variations in pH¹⁶, temperature^{16,17}, or mechanical strain^{18,19} induce changes in d and/or n_{eff} of the PPCs made from a suitably chosen material, thereby eliciting a measurable shift in the value of λ_{sb} .

Decrease in the group velocity of light

Near the edges of the stopband, the group velocity of light decreases because of an increase in the density of light modes^{20,21}. The periodic structure of PPCs can be used to enhance the interaction of light with an active optical component incorporated in the material. For instance, spontaneous emission of a fluorophore in a PPC can be enhanced (or suppressed) as a result of the increased (or decreased) photon density of states, if there is suitable overlap with the emission wavelength of the fluorophore²².

Nonlinear dispersion

Strong anisotropy and nonlinear dispersion (which are not accompanied by loss in photonic crystals) lead to unusually large and highly nonlinear variations in refractive index near the edge of a stopband²³. Therefore, the direction at which light propagates in the crystal is strongly dependent on the wavelength of light. This superprism effect can be used to construct highly sensitive prisms from PPCs.

Fabrication of polymer photonic crystals

Polymer nanostructured materials produced by self-assembly

Self-assembly is the process in which the elements of a system interact in a predetermined way and spontaneously organize to generate a higher order structure²⁴.

Self-assembly of polymer particles (latex or microgel microspheres) into colloid crystals is a typical approach for forming materials with periodic structures. Close-packed colloid crystals (Figs. 2a and 2b) can

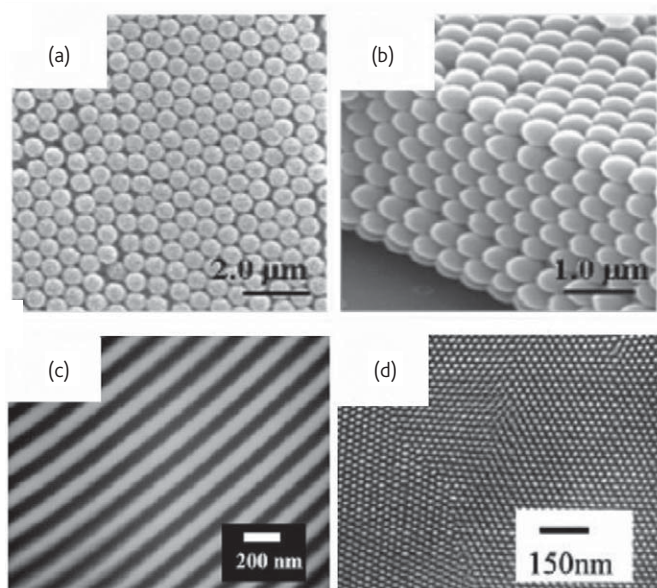


Fig. 2 (a,b) Scanning electron microscopy (SEM) images of a colloid crystal self-assembled from polystyrene particles: (a) top view of the hexagonal close-packed layer of microbeads in the colloid crystal; and (b) cross-sectional view along the depth of the colloid crystal. (Adapted and reprinted with permission from⁵⁵. © 2006 Wiley-VCH.) (c,d) Transmission electron microscopy (TEM) images of cryomicrotomed self-assembled PS-*b*-PI BCP films. The dark regions correspond to PI domains and the bright regions are PS domains. (c) One-dimensional periodic lamellar morphology of PS-*b*-PI films. (Adapted and reprinted with permission from⁴². © 2006 American Chemical Society). (d) Fragment of a triangular array of PS cylinders in a PI matrix. (Adapted and reprinted with permission from⁴³. © 1996 American Chemical Society).

be fabricated using capillary forces²⁵, gravity²⁶, particle assembly on patterned surfaces^{27–29}, and assembly assisted by shear³⁰ or electric and magnetic fields^{31–33}. Unless the formation of one- or two-dimensional colloid crystals is the target, self-assembly typically yields crystals with hexagonal close-packed (hcp) or face-centered cubic (fcc) lattice structures. Alternatively, low volume fraction colloid crystals self-organize in aqueous dispersions owing to the repulsive forces between double electric layers of the particles.

Colloid crystallization is a straightforward and cheap method for producing materials with structural periodicity. However, it has not demonstrated full control over the presence of defects. Enhanced control of crystalline structures comes at a compromised cost, e.g. by depositing microspheres on prepatterned substrates^{34–37}.

The self-assembly of block copolymers (BCPs) is another approach to fabricating nanostructured materials for photonic applications. The simplest BCPs are linear diblock copolymers in which two polymer segments are joined at their endpoints. Different blocks tend to phase separate, but being restricted by their connectivity, they segregate into microdomains with sizes on the order of the dimensions of the respective blocks (~10–100 nm). The organization of BCPs in specific structures, such as spheres on a body-centered cubic lattice,

hexagonal-packed cylinders, double gyroid cubic, or lamellae structures, is determined by the volume and degree of incompatibility of the constituent blocks, as well as the molecular weight, composition, and architecture of the BCPs^{38–41}. Kinetic effects and BCP-substrate interactions provide additional degrees of freedom in controlling BCP structures. Figs. 2c and 2d show representative periodic lamellar and cylindrical structures generated by the self-assembly of a poly(styrene-*b*-isoprene) (PS-*b*-PI) BCP^{42,43}.

Achieving large-area, defect-free periodic structures and particular orientations of anisotropic structures in BCPs requires additional measures, such as tuning film thickness, using topographically and chemically prepatterned substrates, or applying electric and magnetic fields or shear force⁴⁴. On the other hand, some of the defects occurring in BCP films may lead to interesting photonic properties. For instance, point and line defects can act as microcavities and waveguides, respectively⁴⁵. Here, the challenge is in gaining control over the position, type, and directionality of the defects.

Microfabrication of periodic structures in polymer materials

Polymer materials with periodic structures useful for photonic applications can be fabricated by nanoimprinting, photolithography, and sequential deposition of alternating polymer layers.

Nanoimprinting produces topographically patterned polymers by pressing a mold against a softened thermoplastic polymer or a liquid polymer precursor. The resulting surface relief pattern is subsequently trapped by cooling the molded material, or by photocuring the polymer precursor using ultraviolet (UV) light.

In conventional photolithography, periodic structures are produced by (i) selectively exposing a monomer-, or a polymer-coated surface to localized photoirradiation (typically achieved through a mask) and (ii) subsequently removing the selected areas of the polymer film through dissolution in an appropriate solvent. Localized irradiation of a polymer or monomer results in polymerization, cross-linking, or decomposition reactions.

Holographic lithography uses optical interference of laser beams to produce PPCs, and in particular, periodic arrays of LCs dispersed in a polymer matrix^{46,47}. Fabrication of polymer-dispersed LCs is realized via polymerization-induced phase separation. When a mixture of a monomer and a LC is irradiated, polymerization is photoinitiated in areas of high light intensity (defined by the interference pattern of the laser beams), causing phase separation and spatial segregation of LC molecules to areas of low light intensity (Figs. 3a and 3b). The alternating polymer- and LC-rich domains provide a periodic modulation in refractive index in the resulting material^{48–50}.

Two-photon induced polymerization is a powerful approach for the fabrication of three-dimensional microstructures based on computer-generated models⁵¹. As soon as the photon density exceeds a threshold value, simultaneous absorption of two photons by the photosensitive

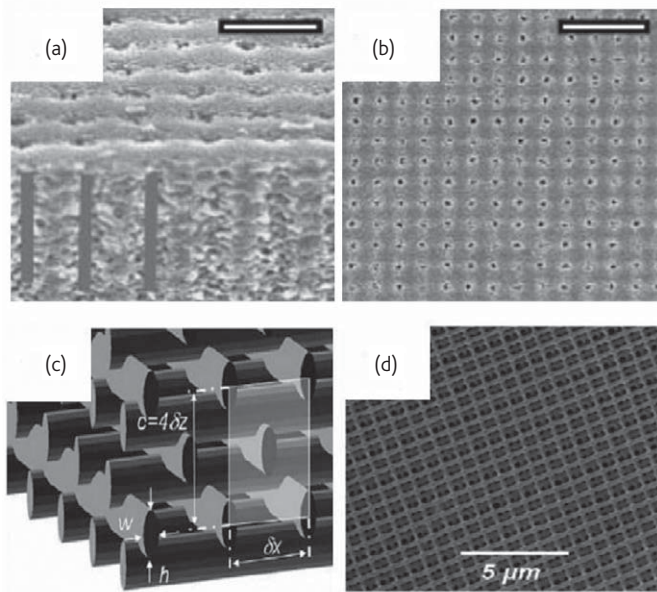


Fig. 3 (a,b) SEM images of a LC-polymer material obtained by holographic patterning of a LC-monomer mixture: (a) cross-sectional and (b) top views. The dark areas are void regions in which the LC droplets resided prior to SEM imaging. Scale bars are (a) 500 nm and (b) 2 μm . (Adapted and reprinted with permission from⁸¹. © 2005 Wiley-VCH). (c,d) Fabrication of materials with periodic structures by two-photon polymerization: (c) computer-generated sketch of a woodpile structure, and (d) SEM image of a woodpile structure fabricated in a resin. (Adapted and reprinted with permission from⁵⁷. © 2006 Elsevier).

resin initiates polymerization within the focal volume. When the focal point is moved in three-dimensional space, polymerization is initiated along the trace of the focus, which allows the fabrication of a broad range of three-dimensional microstructures. A typical woodpile structure generated by two-photon polymerization (Figs. 3c and 3d) has layers of one-dimensional rods with a stacking sequence that repeats itself every four layers⁵¹.

Materials derived from colloid crystals

The majority of photonic applications of colloid crystal-based PPCs make use of a variation in the coherent Bragg scattering from the material occurring in response to external stimuli. Alternatively, diffraction of light by the PPC is used to alter the luminescence of fluorophores (fluorescent dyes or semiconductor nanoparticles) loaded in the PPCs^{52,53}. Fluorophores are incorporated into PPCs by either loading them into polymer microspheres and subsequently self-assembling the hybrid particles into a colloid crystal⁵⁴, or by infiltrating fluorophores into the interstitial voids of the preformed colloid array⁵⁵.

Changes in the spectral position of the stopband originate from a change in the average refractive index and/or the lattice constant of the PPCs, which occurs in response to a change in pH¹⁶, temperature^{16,17}, the presence of analytes (e.g. glucose, Pb^{2+} , Ba^{2+} , K^{+} ions⁹, or biological molecules⁵⁶), electric and magnetic fields^{13–15,57}, and deformation^{8–19,58}. Generally, large variations in the dielectric

constant are required in order to generate modest changes in the spectral position of the stopband, however, notable changes in λ_{sb} can be readily achieved by changing the lattice constant d (see eq 1).

Fig. 4a illustrates the performance of a PPC produced from a colloid crystal embedded in a glucose-recognition material (a polyacrylamide-poly(ethylene glycol) hydrogel with pendant phenylboronic acid groups)⁵⁹. Exposure of this PPC to solutions containing minute concentrations of glucose led to complexation of glucose with the phenylboronic acid moieties and poly(ethylene glycol), a reduction in the hydrogel volume, and hence, a shift in the position of the stopband.

In a second application, deformation applied to elastomeric PPCs changed their lattice constant and caused a shift in the stopband (and hence, the color of diffracted light), as shown in Fig. 4b. The PPCs were fabricated from polymer particles with rigid polystyrene-poly(methyl methacrylate) cores and soft matrix-forming poly(ethyl acrylate) shells⁶⁰. Hysteresis in stretching-contraction series was minimized by cross-linking the poly(ethyl acrylate) matrix.

Electric fields have also been used to tune the stopband of electroactive PPCs^{13–15}. For example, following application of an electric field to a colloid crystal infiltrated with a poly(2-methoxyethyl acrylate) hydrogel loaded with Ag nanoparticles, contraction of the PPC occurred in the plane perpendicular to the plane of electrodes (Fig. 4c, top)¹³. A strong electric-field-induced strain was ascribed to the reorientation of the polar phase in the PPC in response to an electric field (via the electrostrictive effect) and the stress arising from Coulombic interactions between electrostatic charges on the opposing electrodes (via the Maxwell stress effect). The change in interplanar distance of the PPC led to a blue shift of the stopband (Fig. 4c, bottom).

Responsive PPCs can also have the structure of inverse opals^{16,19,61}. For instance, a two-state color switch was obtained using electrochemical means from an inverse opal of a poly(methacrylic acid-co-*N*-isopropylacrylamide) hydrogel¹⁹. In this approach, the electrolysis of water at the anode created an acid and induced shrinkage of the network structure. In another application, an inverse opal of polyacrylamide functionalized with azobenzene moieties showed photoinduced volume changes, and consequently, a shift in the spectral position of the stopband⁶¹.

Polymer nanostructured materials derived from colloid crystals have also been used as recording media for optical data storage⁶². The materials were fabricated by assembling polymer particles with rigid cores comprising of a fluorescent dye and optically inert softer shells into a periodic array. The colloid crystal was subsequently annealed above the glass transition temperature of the shell-forming polymer but below the glass transition temperature of the particle cores⁶³. Under these conditions, the particle shells soften and form a matrix surrounding a periodic array of the fluorescent particles (former cores). Fig. 5a shows the resulting nanostructured material that was used as a

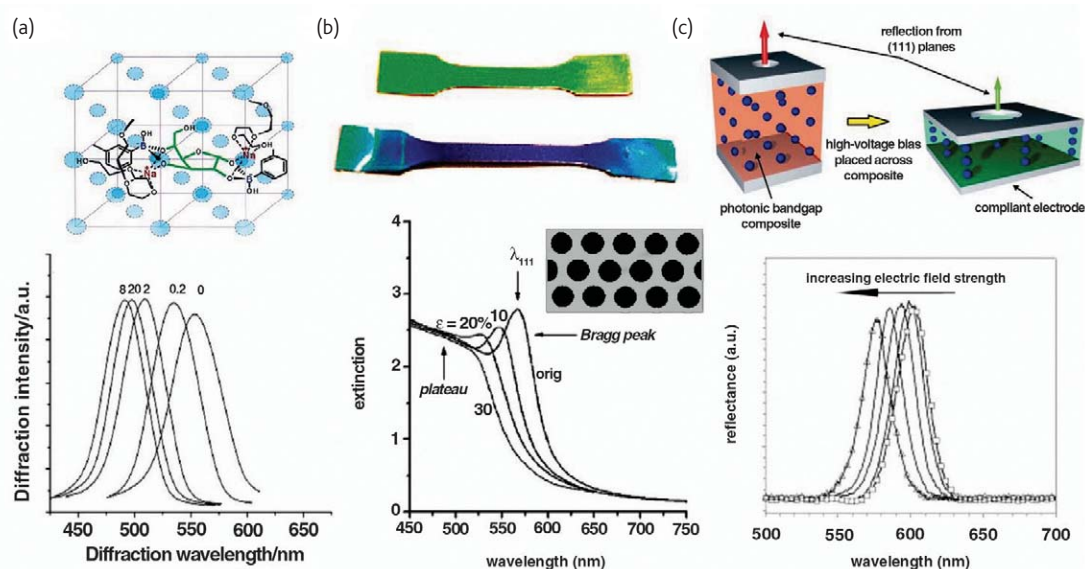


Fig. 4 PPC sensors. (a, top) Schematic of a PPC sensor derived from a colloid crystal embedded in a polyacrylamide-poly(ethylene glycol) hydrogel with pendant phenylboronic acid groups⁵⁹. (bottom) Dependence of the diffraction spectrum of the PPC on the concentration of glucose in an aqueous solution containing 2 mM tris-HCl (pH 8.5) and 150 mM NaCl. Concentration of glucose (in millimolar) is shown next to the corresponding diffraction peaks. (Adapted and reprinted with permission from⁵⁹. © 2003 American Chemical Society.) (b) Deformation of rubbery PPC films obtained from polystyrene-poly(methyl methacrylate)-poly(ethyl acrylate) core-shell particles. (top) Test bars before (green) and after (blue) 200% elongation of the PPC and release. (bottom) UV-visible spectra of the original and deformed rubbery PPC with a cross-linked poly(ethyl acrylate) matrix, where ϵ is elongation and λ_{111} is the spectral position of the Bragg peak. Inset: schematic of the PPC structure. (Adapted and reprinted with permission from⁶⁰. © 2007 American Chemical Society.) (c, top) Schematic of the approach for tuning the position of the stopband in an electroactive PPC. An electric field applied to two flexible electrodes causes contraction of the PPC in the z-direction and decreases the interplanar spacing. (bottom) Reflectance characteristics at normal incidence of an unbiased PPC, consisting of a colloid crystal embedded in a hydrogel of poly(2-methoxyethyl acrylate) loaded with Ag nanoparticles, under electric field strengths up to $25 \text{ V } \mu\text{m}^{-1}$. (Adapted and reprinted with permission from¹³. © 2005 Wiley-VCH.)

medium for high-density, three-dimensional optical data storage⁶². Bits of information were recorded into the material by two-photon-induced photobleaching of the fluorescent 'cores' and, under lower fluence, individually read out (Figs. 5b–5d). The effective optical storage density in the nanostructured material was increased by at least a factor of two relative to homogeneous storage media by spatially localizing the optically active domains and imposing an optically inactive barrier to cross-talk between bits.

A next-generation polymer nanostructured material for optical data recording has been developed for protecting secure documents such as identification documents. The material was fabricated from multilayers of polymer microspheres, which contained UV, visible, and near-infrared fluorescent dyes in the different particle layers^{64,65}. Upon annealing, the outermost, optically inert elastomeric shell of the particles formed a matrix embedding a periodic array of multicolor fluorescent microspheres. Figs. 6a–6c show the structure of the resulting film imaged using excitation wavelengths of 364 nm, 488 nm, and 633 nm (which are close to the absorptions of the three dyes incorporated in the particles). Selective photobleaching of the individual dyes under increased light intensity allowed for the recording of spatially overlapping biometric features – a fingerprint, a photograph, and a signature – with no spectral overlap between them (Figs. 6d–6f). Each pattern was accessed (read) individually

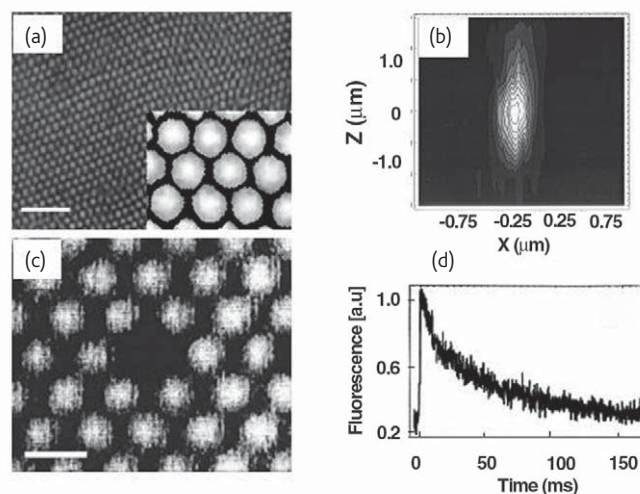


Fig. 5 Polymer nanostructured material for high-density three-dimensional optical memory storage. (a) Confocal fluorescence microscopy image of the material produced from core-shell particles with 500-nm-sized fluorescent cores and 250-nm-thick optically inert shells. Scale bar is 10 μm. Inset: magnified structure of the material. (b) Point spread function of the two-photon beam with dimensions of approximately $0.3 \mu\text{m} \times 0.3 \mu\text{m} \times 1.3 \mu\text{m}$, which was used for recording. (c) Two-photon writing achieved by local photobleaching of the fluorescent dye incorporated into the particle cores. The addressed plane is located 200 μm from the top surface. Scale bar is 1 μm. (d) Fluorescence decay versus time for the addressed particle. (Adapted and reprinted with permission from⁶². © 2001 American Institute of Physics.)

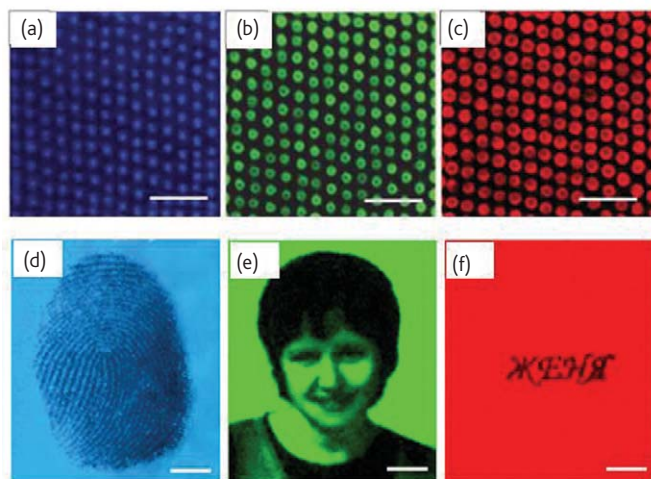


Fig. 6 Recording of biometric features in a polymer nanostructured material derived from multilayer, multidye polymer particles. (a–c) Confocal fluorescence microscopy images of the films examined at a distance 20 μm below the surface using excitation wavelengths, λ_{exc} : (a) 364 nm, (b) 488 nm, and (c) 633 nm. Scale bars are 5 μm . (d–f) Corresponding biometric features recorded in the polymer material by photobleaching the (d) UV, (e) visible, and (f) near-infrared dyes at increased laser intensity. Scale bars are 50 μm . All features are recorded at the same location in the film (10 μm below the top surface). (Adapted and reprinted with permission from⁶⁵. © 2007 Royal Society of Chemistry.)

by irradiating the material at a well-defined wavelength. Since the number of recoding modes scales as 2^n , where n is the number of photosensitizers, recording using three dyes could be achieved in eight distinct modes. The same material has also been used for the recording of full color photographs with different shades of gray⁶⁵.

Materials derived from block copolymers

Band diagrams of all-BCP materials have a plurality of stopbands that do not overlap because of the low dielectric constant mismatch between the phases of the material^{66,67}. This problem has been solved by the selective loading of one of the microphases of BCP films with inorganic nanoparticles (e.g. semiconductor or metal nanoparticles)⁶⁸, or by the selective etching and removal of one of the microphases⁶⁹.

Another challenge in using self-assembled BCP films is to achieve stopbands in the visible spectral range, which implies that the characteristic domain size of a BCP has to be greater than $400/n_d$ where n_d is the refractive index of the material in that domain⁶⁶. Typically, this problem is resolved by swelling one of the microphases of the BCP with a homopolymer or low molecular weight additives^{70–72}. For example, PS-*b*-PI films with different morphologies have been used to fabricate PPCs that diffract in the UV-visible spectral range^{69,73,74}.

Addition of active components to BCPs has been used to render these materials functional and stimuli responsive. Recently, an active optical device was fabricated by confining an organic dye between two lamellae-forming PS-*b*-PI films that act as Bragg reflectors. The BCP reflectors were effective for spectrally selective feedback lasing:

above the lasing threshold, the material showed a sharp lasing peak of 1 nm⁴².

Embedding functional low molecular weight molecules in BCPs has rendered these materials thermo- and electroresponsive. For example, the incorporation of a LC into a lamellar-forming polystyrene-*b*-polymethacrylic acid film allowed the spectral position of the stopband to be shifted through varying the order parameter of the mesogen (and hence the effective refractive index of the BCP) by heating or applying an electric field⁷¹.

In another approach, the reversibility of hydrogen bonding and polymer phase behavior were used to achieve large and reversible temperature-controlled switching of the stopband of a lamellar-forming BCP. A thermal response in the optical properties of polystyrene-*b*-poly(4-vinylpyridinium methanesulphonate), or PS-*b*-P4VP(MSA), was induced by adding 3-*n*-pentadecylphenol (PDP) to the BCP (Figs. 7a and 7b)⁷⁵. Below $\sim 125^\circ\text{C}$, a complex of PS-*b*-P4VP(MSA) with PDP produced a supramolecular comb-shaped architecture with a long lamellar period (Fig. 7a). The sample is green, birefringent, and had a lamellar structure (Fig. 7c). Above 125°C , the hydrogen bonds broke up and PDP dissolved in both PS and P4VP(MSA), leading to a sharp, reversible transition to an uncolored and non-birefringent material (Fig. 7d). An abrupt change in the BCP structure led to a change in UV-visible specular transmission and diffuse reflectance (Figs. 7e–7g).

Microfabricated polymer photonic crystals

Although holographic patterning is a convenient method of forming complex three-dimensional structures from photoresists^{76,77}, it is more commonly used to fabricate photonic devices from holographically patterned polymer-dispersed liquid crystals (H-PDLCs). Since polymers and LCs have a modest difference in refractive index (typically, $\Delta n \leq 0.2$), most H-PDLC-based devices exploit the low group velocity of light, which is developed near the edges of the bandgap^{78–81}.

For example, the emission of a fluorophore incorporated into a H-PDLC structure can be amplified, if there is an overlap between the emission of the fluorophore and the edge of the stopband. The resulting increase in the interaction of light with the fluorophore leads to coherent feedback and lasing once a threshold is reached⁸⁰. Using this concept, lasing has been demonstrated for two-dimensional H-PDLC structures, in which the lasing wavelength was modulated by applying an electric field⁸¹.

In another example, opto-control of light reflection has been achieved in a one-dimensional H-PDLC (Fig. 8)⁸². The H-PDLC structure had alternating layers of primary LC molecules possessing nematic order and secondary LC molecules that underwent a UV-triggered *trans-cis* photoisomerization. When the material was exposed to UV irradiation, the photoisomerization of the secondary LC molecules disrupted the nematic order of the primary LC molecules and induced a refractive index mismatch in the photonic structure. The mismatch

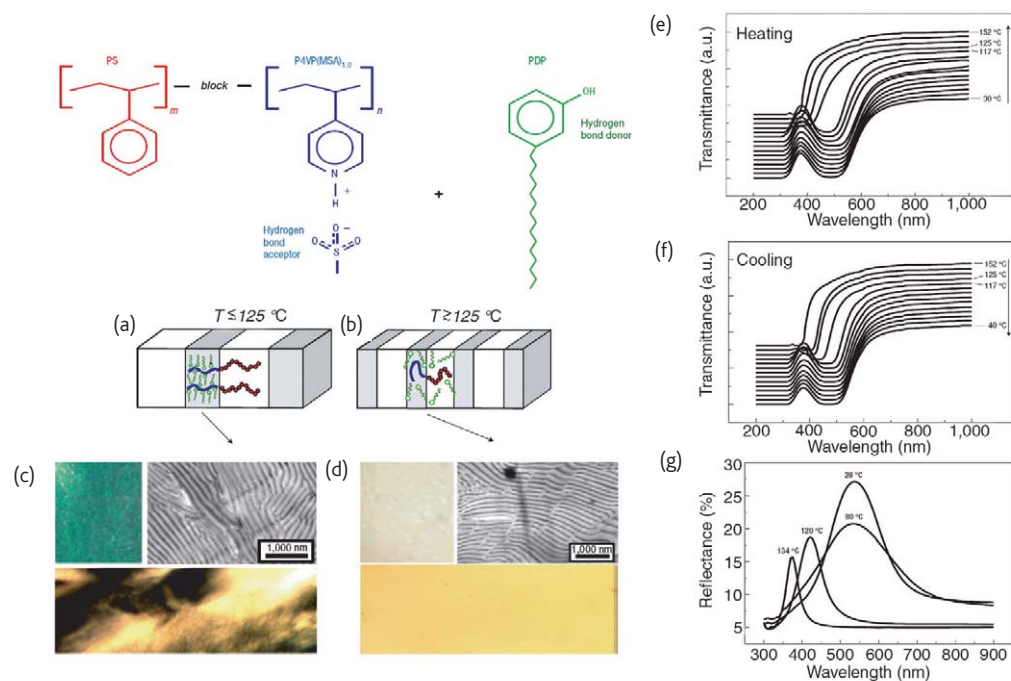


Fig. 7 Properties of PS-*b*-P4VP(MSA) mixed with PDP at room temperature and at $\sim 125^\circ\text{C}$. (a) At room temperature, PDP is a selective solvent for P4VP(MSA) and the sample has structural hierarchy. (b) At $\sim 125^\circ\text{C}$, PDP is a solvent for both PS and P4VP(MSA), and the internal structure within the P4VP(MSA)-containing domains disappears. (c) At room temperature, the sample is green, has a lamellar structure and a birefringent texture (observed up to $\sim 125^\circ\text{C}$). (d) At $> 125^\circ\text{C}$, the material is uncolored, has a lamellar structure when rapidly quenched from 170°C , and is non-birefringent. (e, f) Variation in the UV-visible specular transmission of the material following (e) heating and (f) cooling of the samples. (g) Material response observed in reflectance measurements. (Reprinted with permission from⁷⁵. © 2004 Nature Publishing Group.)

produced a stopband and hence, a decrease in the transmission at the diffraction wavelengths.

Polymer materials comprising long cylinders of nematic LCs have also been used to realize a superprism effect⁸³. These H-PDLC photonic crystals possessed a refractive index mismatch of 0.2, which was sufficient for strong dispersion of light. When the sample was illuminated with white light at the normal of the PPC, the angle of the deflected light showed a strong dependence on

wavelength: light at 450 nm and 680 nm was deflected at 53° and 90° , respectively.

Patterning of photoresists by means of multiphoton polymerization has generated novel sophisticated structures in PPCs. Fig. 9 shows right- and left-handed three-dimensional spiral photonic crystals fabricated by direct laser writing in SU-8 photoresist⁸⁴. The resulting PPCs gave rise to strong circular dichroism: the transmission of light was 5% and 95% for different incident circular

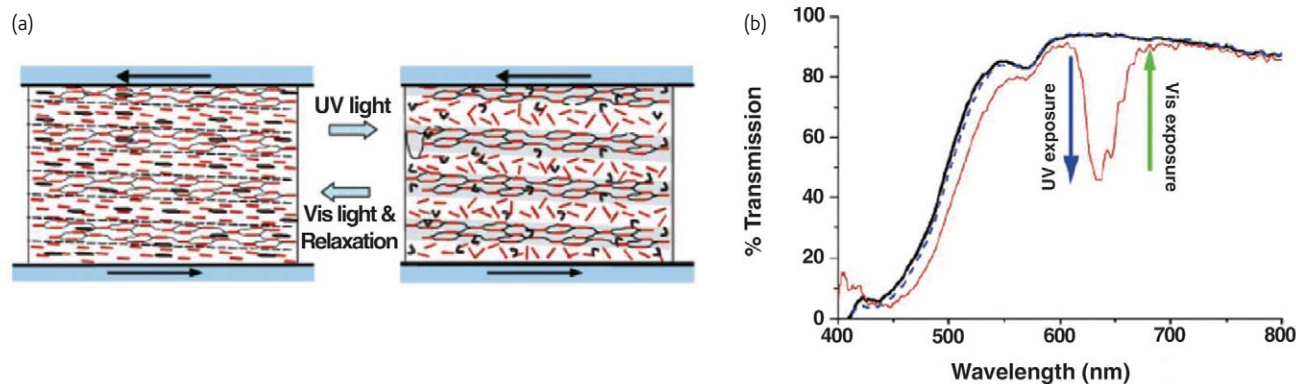


Fig. 8 (a) Schematic of an H-PDLC multilayered polymer reflector. Layers of LCs in a planar arrangement and immobilized by a polymer network alternate with layers of LCs droplets stabilized by a polymer. Upon UV irradiation, a secondary LC (shown in black) in the unconstrained layer undergoes trans-cis photoisomerization, disrupting the nematic order of the host LC (shown in red). (b) The material shows high transmission prior to UV irradiation (black curve) and low transmission after UV irradiation (red curve). The dashed curve shows the transmission of the reflector after the secondary LCs have relaxed back to the trans form. (Adapted and reprinted with permission from⁸². © 2004 American Chemical Society.)

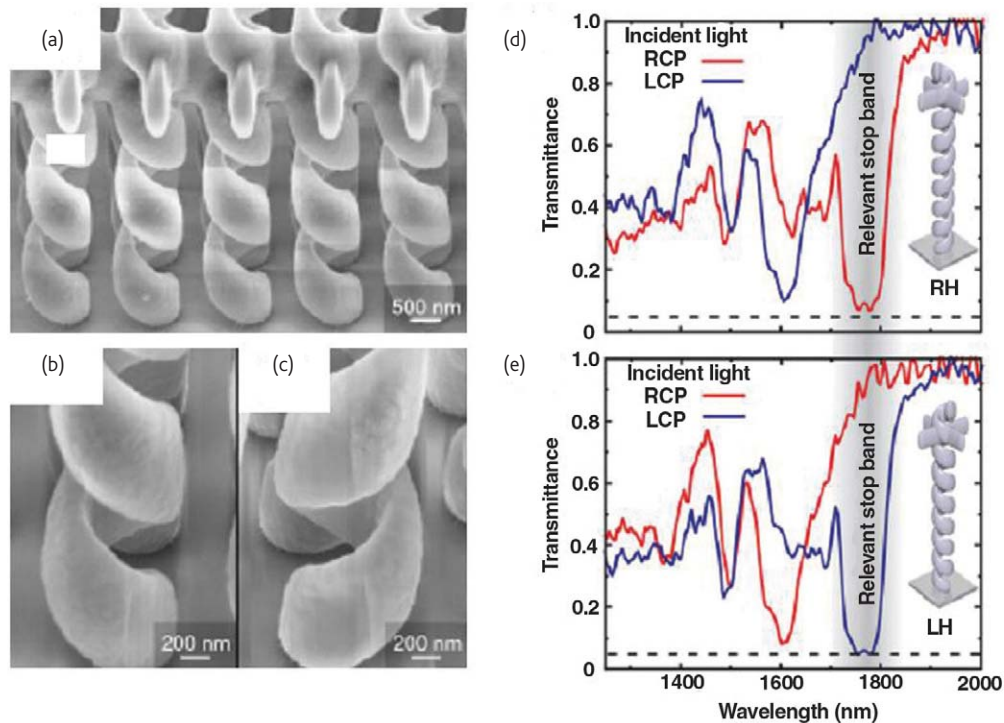


Fig. 9 (a) SEM image of a chiral PPC fabricated by direct multiphoton laser writing. Close-ups of (b) left- and (c) right-handed spirals. (d) Transmission of the right-handed three-dimensional spiral photonic crystal. At $\lambda = 1.8 \mu\text{m}$, the transmittance in the right-handed crystal is low for right circularly polarized light (RCP, red), and high for left circularly polarized light (LCP, blue). (e) Transmission of the left-handed spiral photonic crystal. The same trend exists for the left-handed crystal, but with reversed sense of rotation of circularly polarized light. (Adapted and reprinted with permission from⁸⁴. © 2007 Wiley-VCH.)

polarizations⁸⁴. For example, the transmittance in the right-handed PPC was low for right circularly polarized light and high for left circularly polarized light.

Direct laser writing by multiphoton polymerization has also been identified as a powerful technique for controllably incorporating defects into PPCs^{85–88}. For instance, two-photon polymerization has been used for the incorporation of predefined features within self-assembled photonic crystals^{85–87} and within holographically patterned, three-dimensional PPCs⁸⁸.

Outlook

Owing to the ability to combine structure- and composition-dependent properties, the scope of research in polymer nanostructured materials with periodic structures has rapidly expanded beyond traditional polymer nanocomposites for optical applications. Future advances in this area of science and technology will aim at improving the photonic functionalities of polymer materials, controlling structural defects, and integrating photonic devices.

Development of polymer materials for photonic applications will include the synthesis of polymers with high refractive indexes and/or useful optical and electronic properties (for instance, using inorganic polymers⁸⁹), the use of optically active hybrid polymer-inorganic materials, and the utilization of materials with multiple sensing functions. Specific functionalities of polymers and rapid dynamic


response to particular, and sometimes multiple, external stimuli will serve as another criterion for the successful commercialization of photonic polymer materials.

Polymer nanostructured materials for secure data storage is another field of research that holds promise, with an increasing demand for the protection of identification documents, credit cards, and authentication labels against counterfeiting. Here, future advances depend on the synthesis of photostable chromophores, the incorporation of multiple security features in polymer recording media, and the ability to integrate polymer security materials with cost-effective optical reading devices.

The challenge in controlling defects in polymer materials with periodic structures involves the assembly or fabrication of large-area materials with close-to-perfect crystalline structures and/or the introduction of predefined site-specific defects. Polymer materials for defect-tolerant applications such as photonic sensing are likely to be produced by self-assembly techniques, which are cost-effective and can be used for applying materials to substrates with arbitrary shapes. Microfabricated polymer systems have the advantage of precise control over their structures and the ability to introduce new symmetries and predefined features in the PPCs. The challenges include the high cost and relatively low throughput of currently used microfabrication techniques. Applications of such materials include photonic-crystal fiber optics and the fabrication of superprisms, antireflective coatings, and

high-precision optical filters and mirrors. The challenges in introducing defects in three-dimensional crystal structures can potentially be addressed by combining fabrication techniques, e.g. holography with electron-beam lithography, or self-assembly with two-photon polymerization.

Finally, current challenges in device integration include the ability to combine PPC devices with other optoelectronic components or to couple them to optical waveguides. The use of PPCs (compared with

their semiconductor counterparts) for reduced power dissipation, higher bandwidths in communication links, lasing, and optical computing will strongly depend on the development of polymer materials with suitable optical, mechanical, and thermal properties, and fine tuning of the structure of PPCs. 

Acknowledgments

The authors thank Hendrick De Haan for help with the illustrations.

REFERENCES

- Jiang, H. Y., et al., *Adv. Mater.* (2006) **18**, 1471
- Lindsay, G. A., et al., *Mater. Sci. Eng. B* (2006) **132**, 8
- Xia, Y., et al., *Adv. Mater.* (2001) **13**, 409
- Braun, P. V., et al., *Adv. Mater.* (2006) **18**, 2665
- López, C., *Adv. Mater.* (2003) **15**, 1679
- Joannopoulos, J. D., *Nature* (2001) **414**, 257
- Fudouzi, H., and Xia, Y., *Adv. Mater.* (2003) **15**, 892
- Bertolotti, M., *J. Opt. A: Pure Appl. Opt.* (2006) **8**, 59
- Holtz, J. H., and Asher, S. A., *Nature* (1997) **389**, 829
- Asher, S. A., et al., *Anal. Chem.* (2003) **75**, 1676
- Ben-Moshe, M., et al., *Anal. Chem.* (2006) **78**, 5149
- Kimble, K. W., et al., *Anal. Bioanal. Chem.* (2006) **385**, 678
- Xia, J., et al., *Adv. Mater.* (2005) **17**, 2463
- Arsenault, A. C., et al., *Nat. Photon.* (2007) **1**, 468
- Arsenault, A. C., et al., *Adv. Mater.* (2003) **15**, 503
- Ueno, K., et al., *Adv. Mater.* (2007) **19**, 2807
- Debord, J. D., et al., *Adv. Mater.* (2002) **14**, 658
- Pursiainen, O. L. J., et al., *Appl. Phys. Lett.* (2005) **87**, 101902
- Arsenault, A. C., et al., *Nat. Mater.* (2006) **5**, 179
- Dowling, J. P., et al., *J. Appl. Phys.* (1994) **75**, 1896
- Sakoda, K., *Opt. Express* (1999) **4**, 167
- Soljačić, M., and Joannopoulos, J. D., *Nat. Mater.* (2004) **3**, 211
- Lin, S.-Y., et al., *Opt. Lett.* (1996) **21**, 1771
- Parviz, B. A., et al., *IEEE Trans. Adv. Pack.* (2003) **26**, 233
- Jiang, P., and McFarland, M. J., *J. Am. Chem. Soc.* (2004) **126**, 13778
- Mayoral, R., et al., *Adv. Mater.* (1997) **9**, 257
- van Blaaderen, A., et al., *Nature* (1997) **385**, 321
- Golding, R. K., et al., *Langmuir* (2004) **20**, 1414
- Allard, M., et al., *Adv. Mater.* (2004) **16**, 1360
- Vickreva, O., et al., *Adv. Mater.* (2000) **12**, 110
- Trau, M., et al., *Science* (1996) **272**, 706
- Rogach, A. L., et al., *Chem. Mater.* (2000) **12**, 2721
- Helseth, L. E., et al., *Langmuir* (2004) **20**, 7323
- Lu, Y., et al., *Langmuir* (2001) **17**, 6344
- Park, S. H., and Xia, Y., *Adv. Mater.* (1998) **10**, 1045
- Kumacheva, E., et al., *Adv. Mater.* (2002) **14**, 221
- Míguez, H., et al., *Appl. Phys. Lett.* (2002) **81**, 2493
- Li, M., and Ober, C. K., *Materials Today* (2006) **9** (9), 30
- Fasolka, M. J., and Mayes, A. M., *Annu. Rev. Mater. Res.* (2001) **31**, 323
- Yoon, J., et al., *MRS Bull.* (2005) **30**, 721
- Hamley, I. W., *Nanotechnology* (2003) **14**, R39
- Yoon, J., et al., *Nano Lett.* (2006) **6**, 2211
- Honeker, C. C., and Thomas, E. L., *Chem. Mater.* (1996) **8**, 1702
- Angelescu, D. E., et al., *Adv. Mater.* (2004) **16**, 1736
- Mekis, A., et al., *Phys. Rev. Lett.* (1996) **77**, 3787
- Escuti, M. J., and Crawford, G. P., *Opt. Eng.* (2004) **43**, 1973
- Bunning, T. J., et al., *Annu. Rev. Mater. Res.* (2000) **30**, 83
- Escuti, M. J., et al., *Opt. Lett.* (2003) **28**, 522
- Sutherland, R., et al., *Opt. Express* (2002) **10**, 1074
- Escuti, M. J., et al., *Appl. Phys. Lett.* (2003) **83**, 1331
- Wu, S., et al., *J. Photochem. Photobiol. A: Chem.* (2006) **181**, 1
- Evanoff, D. D., Jr., et al., *Adv. Mater.* (2007) **19**, 3507
- Lin, Y., et al., *Appl. Phys. Lett.* (2002) **81**, 3134
- Xu, S., et al., *Adv. Funct. Mater.* (2003) **13**, 468
- Paquet, C., et al., *Adv. Funct. Mater.* (2006) **16**, 1892
- Cassagneau, T., and Caruso, F., *Adv. Mater.* (2002) **14**, 1629
- Ge, J., et al., *Angew. Chem. Int. Ed.* (2007) **46**, 7428
- Finkelmann, H., et al., *Adv. Mater.* (2001) **13**, 1069
- Alexeev, V., et al., *Anal. Chem.* (2003) **75**, 2316
- Viel, B., et al., *Chem. Mater.* (2007) **19**, 5673
- Matsubara, K., et al., *Angew. Chem. Int. Ed.* (2007) **46**, 1688
- Siwick, B. J., et al., *J. Appl. Phys.* (2001) **90**, 5328
- Kalinina, O., and Kumacheva, E., *Macromolecules* (1999) **32**, 4122
- Pham, H. H., et al., *Adv. Mater.* (2004) **16**, 516
- Pham, H. H., et al., *J. Mater. Chem.* (2007) **17**, 523
- Fink, Y., et al., *J. Lightwave Technol.* (1999) **17**, 1963
- Edrington, A. C., et al., *Adv. Mater.* (2001) **13**, 421
- Bockstaller, M. R., and Thomas, E. L., *J. Phys. Chem. B* (2003) **107**, 10017
- Urbas, A. M., et al., *Adv. Mater.* (2002) **14**, 1850
- Urbas, A., et al., *Adv. Mater.* (2000) **12**, 812
- Osuji, C., et al., *Adv. Funct. Mater.* (2002) **12**, 753
- Kang, Y., et al., *Nat. Mater.* (2007) **6**, 957
- Urbas, A., et al., *Macromolecules* (1999) **32**, 4748
- Deng, T., et al., *Polymer* (2003) **44**, 6549
- Valkama, S., et al., *Nat. Mater.* (2004) **3**, 872
- Jang, J.-H., et al., *Adv. Funct. Mater.* (2007) **17**, 3027
- Moon, J., et al., *Opt. Express* (2005) **13**, 9841
- Lucchetta, D. E., et al., *Appl. Phys. Lett.* (2004) **84**, 4893
- Jakubiak, R., et al., *Adv. Mater.* (2003) **15**, 241
- Jakubiak, R., et al., *Appl. Phys. Lett.* (2004) **85**, 6095
- Jakubiak, R., et al., *Adv. Mater.* (2005) **17**, 2807
- Urbas, A., et al., *J. Am. Chem. Soc.* (2004) **126**, 13580
- Li, M. S., et al., *Appl. Phys. Lett.* (2006) **88**, 091109
- Thiel, M., et al., *Adv. Mater.* (2007) **19**, 207
- Lee, W., et al., *Adv. Mater.* (2002) **14**, 271
- Jun, Y., et al., *Adv. Mater.* (2005) **17**, 1908
- Pruzinsky, S. A., and Braun, P. V., *Adv. Funct. Mater.* (2005) **15**, 1995
- Scrimgeour, J., et al., *Adv. Mater.* (2006) **18**, 1557
- Paquet, C., et al., *Chem. Mater.* (2004) **16**, 5205